REPORT DOCUMENTATION PAGE

Form Approved OMB NO. 0704-0188

1. REPORT DATE (DD-MM-YYYY)	2. REPORT TYPE	3. DATES COVERED (From - To)
	New Reprint	-

4. TITLE AND SUBTITLE

Infrared Spectra and Binding Energies of Chemical Warfare Nerve Agent Simulants on the Surface of Amorphous Silica

5a. CONTRACT NUMBER	W911NF-06-1-0111
5b. GRANT NUMBER	
5c. PROGRAM ELEMENT NUMBER	106013
5d. PROJECT NUMBER	
5e. TASK NUMBER	
5f. WORK UNIT NUMBER	

6. AUTHORS

Wesley O. Gordon, Erin Durke Davis, Diego Troya, Brent A. Mantooth, Amanda R. Wilmsmeyer, Teri A. Lalain, John R. Morris

7. PERFORMING ORGANIZATION NAMES AND ADDRESSES

Virginia Polytechnic Institute & State University
Office of Sponsored Programs
1880 Pratt Drive, Suite 2006
Blacksburg, VA 24060 -3580

8. PERFORMING ORGANIZATION REPORT NUMBER

9. SPONSORING/MONITORING AGENCY NAME(S) AND ADDRESS(ES)

U.S. Army Research Office
P.O. Box 12211
Research Triangle Park, NC 27709-2211

10. SPONSOR/MONITOR'S ACRONYM(S)
ARO

11. SPONSOR/MONITOR'S REPORT NUMBER(S)
49379-CH.8

12. DISTRIBUTION AVAILIBILITY STATEMENT

Approved for public release; distribution is unlimited.

13. SUPPLEMENTARY NOTES

The views, opinions and/or findings contained in this report are those of the author(s) and should not contrued as an official Department of the Army position, policy or decision, unless so designated by other documentation.

14. ABSTRACT

The fundamental interactions of a series of chemical warfare agent (CWA) simulants on amorphous silica particulates have been investigated with transmission infrared spectroscopy and temperature-programmed desorption (TPD). The simulants methyl dichlorophosphate (MDCP), dimethyl cholorophosphate (DMCP), trimethyl phosphate (TMP), dimethyl methylphosphonate (DMMP), and diisopropyl methylphosphonate (DIMP) were chosen to help develop a comprehensive understanding for how the structure and functionality of CWA

15. SUBJECT TERMS

chemical warfare agent, silica, binding energies, temperature programmed desorption, infrared spectroscopy

16. SECURITY CLASSIFICATION OF:			17. LIMITATION OF ABSTRACT	15. NUMBER OF PAGES	19a. NAME OF RESPONSIBLE PERSON
a. REPORT	b. ABSTRACT	c. THIS PAGE			John Morris
UU	UU	UU	UU		19b. TELEPHONE NUMBER: 540-231-2472

Report Title

Infrared Spectra and Binding Energies of Chemical Warfare Nerve Agent Simulants on the Surface of Amorphous Silica

ABSTRACT

The fundamental interactions of a series of chemical warfare agent (CWA) simulants on amorphous silica particulates have been investigated with transmission infrared spectroscopy and temperature-programmed desorption (TPD). The simulants methyl dichlorophosphate (MDCP), dimethyl cholorophosphate (DMCP), trimethyl phosphate (TMP), dimethyl methylphosphonate (DMMP), and diisopropyl methylphosphonate (DIMP) were chosen to help develop a comprehensive understanding for how the structure and functionality of CWA surrogate compounds affect uptake and hydrogen-bond strengths at the gas-surface interface. Each simulant was found to adsorb molecularly to silica through the formation of strong hydrogen bonds primarily between isolated surface silanol groups and the oxygen atom of the P=O moiety in the adsorbate. The TPD data revealed that the activation energy for desorption of a single simulant molecule from amorphous silica varied slightly with coverage. In the limit of zero coverage and the absence of significant surface defects, the activation energies for desorption were found to follow the trend: MDCP < DMCP < TMP < DMMP < DIMP. This trend demonstrates the critical role of electron withdrawing substituents in determining the adsorption energies through hydrogen-bonding interactions. The infrared spectra for each adsorbed species, recorded during uptake, showed a significant shift in the frequency of the ?(SiO-H) mode as the hydrogen bonds formed. A clear linear relationship between the desorption energy and the shift of the surface ?(SiO-H) mode across this series of adsorbates demonstrates that the Badger-Bauer relationship, established origninally for solute-solvent interactions, effectively extends to gas-surface interactions. High-level electronic structure calculations, including extrapolation to the complete basis set limit, reproduce the experimental energies of all simulants with high levels of accuracy and have been employed to provide insight into the molecular-level details of adsorption geometries for the simulants, and to predict the interaction energies for the CWA, isopropyl methylphosphonofluoridate (sarin).

REPORT DOCUMENTATION PAGE (SF298)
(Continuation Sheet)

Continuation for Block 13

ARO Report Number 49379.8-CH
Infrared Spectra and Binding Energies of Chemi ...

Block 13: Supplementary Note

Approved for public release; distribution is unlimited.

THE JOURNAL OF PHYSICAL CHEMISTRY C

Article

pubs.acs.org/JPCC

Infrared Spectra and Binding Energies of Chemical Warfare Nerve Agent Simulants on the Surface of Amorphous Silica

Amanda R. Wilmsmeyer,[†] Wesley O. Gordon,[‡] Erin Durke Davis,[§] Diego Troya,[†] Brent A. Mantooth,[‡] Teri A. Lalain,[‡] and John R. Morris*[,†]

[†]Department of Chemistry, Virginia Tech, Blacksburg, Virginia 24061, United States

[‡]Research and Technology Directorate, Edgewood Chemical Biological Center, Edgewood, Maryland 21010, United States

[§]Optimetrics, Inc./DCS Corp, Abingdon, Maryland 21009, United States

ABSTRACT: The fundamental interactions of a series of chemical warfare agent (CWA) simulants on amorphous silica particulates have been investigated with transmission infrared spectroscopy and temperature-programmed desorption (TPD). The simulants methyl dichlorophosphate (MDCP), dimethyl cholorophosphate (DMCP), trimethyl phosphate (TMP), dimethyl methylphosphonate (DMMP), and diisopropyl methylphosphonate (DIMP) were chosen to help develop a comprehensive understanding for how the structure and functionality of CWA surrogate compounds affect uptake and hydrogen-bond strengths at the gas−surface interface. Each simulant was found to adsorb molecularly to silica through the formation of strong hydrogen bonds primarily between isolated surface silanol groups and the oxygen atom of the P═O moiety in the adsorbate. The TPD data revealed that the activation energy for desorption of a single simulant molecule from amorphous silica varied slightly with coverage. In the limit of zero coverage and the absence of significant surface defects, the activation energies for desorption were found to follow the trend MDCP < DMCP < TMP < DMMP < DIMP. This trend demonstrates the critical role of electron-withdrawing substituents in determining the adsorption energies through hydrogen-bonding interactions. The infrared spectra for each adsorbed species, recorded during uptake, showed a significant shift in the frequency of the ν(SiO−H) mode as the hydrogen bonds formed. A clear linear relationship between the desorption energy and the shift of the surface ν(SiO−H) mode across this series of adsorbates demonstrates that the Badger−Bauer relationship, established originally for solute−solvent interactions, effectively extends to gas−surface interactions. High-level electronic structure calculations, including extrapolation to the complete basis set limit, reproduce the experimental energies of all simulants with high levels of accuracy and have been employed to provide insight into the molecular-level details of adsorption geometries for the simulants and to predict the interaction energies for the CWA isopropyl methylphosphonofluoridate (sarin).

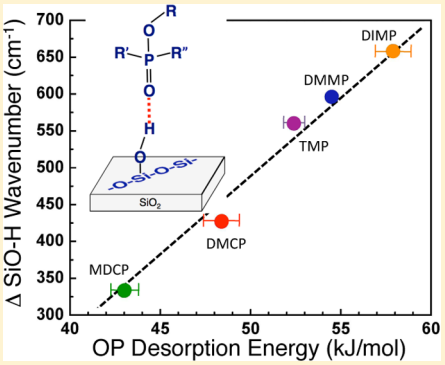

I. INTRODUCTION

Detailed insight into the surface chemistry of chemical warfare agents (CWAs) is critical to the rational design of advanced filters, sorbents, and decontamination strategies for these extremely toxic compounds. A great deal of research into the interactions of CWA simulants, less toxic surrogates for the actual agents, on surfaces has been performed recently;[1] however, there remains a poor understanding for how the chemical properties of the simulants and agents affect the overall surface chemistry. In an effort to more fully elucidate how the structure and functionality of common simulants for the nerve agent sarin affect fundamental aspects of binding to surfaces, we have initiated a study into the uptake and binding of a series of organophosphorus (OP) molecules to the surface of silica, one of the most abundant materials in environmental and industrial settings and an excellent test system for exploring gas−surface hydrogen-bonding interactions.

The surfaces of many metal and metal-oxide materials are composed of a native oxide layer that rapidly forms when the fresh material is exposed to atmospheric oxygen and water. The oxide layer often passivates the material against further oxidation.[2] However, the layer typically contains hydroxyl groups that serve as binding sites for polar gas-phase species. In particular, the phosphoryl group of CWAs and their simulants has been shown to initially bond to several types of metal oxides through the formation of hydrogen-bonding interactions to the surface hydroxyl groups.[3−26] Drawing inspiration from these earlier studies, we have explored the fundamental nature of hydrogen-bonding interactions of CWA simulants on the surface of silica. Silica surfaces are ideal substrates on which to explore the details of gas−surface hydrogen-bonding interactions because the hydroxyl coverage on the surface can be controlled, the material is relatively inert toward reactions, and the surface has been well characterized in previous work.[4,7,11,27−30]

Received: April 30, 2013
Revised: June 20, 2013
Published: June 24, 2013

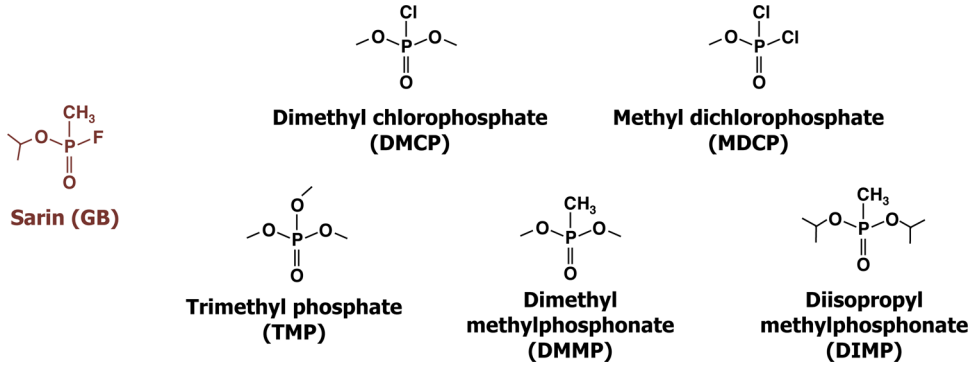

Figure 1. Composition of the nerve agent sarin and five common simulants.

The structures of several possible simulants for the nerve agent sarin are shown in Figure 1. Similar to sarin, they all possess a central ester moiety, but they differ from the agent in that they do not bind well to the active site in acetylcholinesterase,[1] thereby significantly reducing their toxicity. The most commonly used simulant, dimethyl methylphosphonate (DMMP), is very similar in vapor pressure to sarin; however, DMMP lacks the bulky isopropyl group of sarin and the small fluorine substituent, which are key chemical features that likely have a significant effect on the overall surface chemistry. The other simulants likewise lack important features of the agent that limit one's ability to accurately predict the surface chemistry of the agent without a comprehensive understanding for how the structure and functionality affect the outcome of the molecule−surface interactions.

Organophosphonate adsorption on silica has been studied experimentally[5,6,11,23,26,27,31] and theoretically.[7,11,23,28] Some of the first studies into the adsorption of the simulant dimethyl methylphosphonate (DMMP) to silica, performed by Henderson and co-workers, concluded that very strong hydrogen-bonding interactions govern molecular adsorption.[27] Further work by Kanan and Tripp employed infrared spectroscopy to demonstrate that the strength of DMMP−silica interactions depends on the number of hydrogen bonds that may be formed with the surface.[31] They indicated that DMMP adsorption could occur via hydrogen bonding to the sp^3 oxygen atoms of the methoxy groups and the sp^2 oxygen bound to the central phosphorus atom. Beyond these experimental studies, Bermudez used quantum chemical calculations to explore the adsorption of DMMP and sarin on silica.[7] Those studies concluded that hydrogen bonding between the sp^2-hybridized oxygen atom and two surface hydroxyls was the dominant interaction driving adsorption. In addition, Quenneville et al. employed computational methods to study the influence of surface hydration on the DMMP−silica interaction and showed that the hydroxyl surface density strongly affected the resulting adsorbed species.[28] Most recently, Wilmsmeyer et al. performed experiments to directly compare the desorption energies of DMMP and the halogenated OP molecule DMCP.[26] They found that the electron-withdrawing Cl functional group reduced the OP desorption energy relative to the non-halogenated compound. Nadler et al. also investigated the effect of halogenation on surface interactions by studying the adsorption of diisopropyl fluorophosphate (DFP) on silica. Their work indicated that the dominant interaction pathway was through molecular adsorption.[32]

Perhaps most relevant to the current work, Taylor et al.[23] reported a combined theoretical and experimental study in which they investigated the adsorption of DMMP, DIMP, DFP, and sarin to silica at high temperatures. Density functional theory was used to compute vibrational spectra and adsorption energies that capture experimental measurements carried out via inverse gas chromatography at temperatures in the 413−473 K range. In that work, calculations of adsorption energies on various potential surface sites, including isolated, vicinal, and geminal silanols, were performed. While they found good agreement between experimental and theoretical binding energies for the molecules DIMP and sarin, sizable differences between theory and experiment were revealed for other molecules such as DMMP and DFP.

While many groups have investigated the fundamental interactions between select organophosphorous compounds and silica, many questions remain. The adsorption energy of DMMP, for example, on silica has been reported as 54.5,[26] 56.9,[7] 70.7,[27] 83.7,[7] and 109.2[23] kJ/mol depending on the adsorption structure and method of analysis. In addition to this variation of adsorption strength for one simulant, only a very qualitative analysis of the relative adsorption strength of different simulants has been reported. The work described below was designed to provide quantitative experimental determination of the desorption energies for the five simulants shown in Figure 1 on amorphous particulate silica. By tracking the molecule−surface interactions for these compounds, which differ by key substituents, we aim to provide insight into the fundamental details of interfacial hydrogen bonding. In addition to serving as a needed benchmark for high-level theoretical studies, these results can be used to help predict how halogen substituents within organophosphorous compounds (a key characteristic of the CWAs sarin and soman[7]) affect the strength of hydrogen-bond formation on silica. We have pursued these objectives by performing a series of temperature-programmed desorption (TPD) measurements to determine the activation energy for desorption of the simulants. Surface-sensitive infrared spectroscopy was utilized to help reveal how the vibrational modes of the surface and the simulants are affected by adsorption. In addition, quantum chemical (QC) calculations were performed to provide a molecular-level understanding of the bonding geometries and electronic structure of the organophosphorous compounds on silica. Furthermore, the calculations enable us to explore chemistry beyond the simulant molecules and learn how the actual agent sarin binds to silica. Through these observations, we have begun to learn about the key functional groups involved in the uptake of the molecules on a silica surface.

dx.doi.org/10.1021/jp404265s | J. Phys. Chem. C 2013, 117, 15685−15697

II. EXPERIMENTAL SECTION

Experiments were conducted in an ultrahigh vacuum (UHV) chamber with a base pressure of 10^{-10} Torr. An important benefit of performing the experiments in UHV is that contaminants that can establish hydrogen bonds with the simulants or surface silanol groups, especially water, have very low concentrations. Silica samples were prepared by pressing approximately 5 mg of silica nanoparticles (Aerosil, 200 m^2/g, 12 nm average particle diameter) into a 50 μm thick tungsten mesh grid (Tech-Etch) that could be resistively heated and cooled. Immediately prior to each experiment, the sample was annealed for 5 min at 700 K, as monitored by a type K thermocouple spot-welded to the top of the mesh. Based on similar nanoparticle types, this sample pretreatment process produces a surface hydroxyl density of 2.0 OH/nm^2.[29,30] The sample was then cooled by filling the sample reservoir with liquid nitrogen (Airgas) until a surface temperature of 225 K was reached.

DMMP (97%), TMP (99+%), DMCP (96%), and MDCP (85%) were purchased from Sigma-Aldrich. DIMP (95%) was purchased from Alfa-Aesar. All simulants were purified via three freeze−pump−thaw cycles prior to use. These simulants were stored in glass bulbs attached to bellows-sealed valves welded on a stainless steel manifold. Simulant dosing was achieved using a stainless steel directional doser with a glass capillary array positioned 2 mm from the center of the silica sample spot.

IR Data Acquisition. Transmission IR spectroscopy was performed with a Nicolet Nexus 670 FTIR spectrometer coupled to the UHV chamber. Each spectrum was the average of 128 scans collected at 4 cm^{-1} resolution, with a 32 mm aperture and 1.89 cm/s scanner velocity. The spectra presented in this work are shown as difference spectra. For characterization of the silica sample itself, a blank spot on the mesh was used to provide a reference spectrum. For surface characterization during dosing, a spectrum of the clean silica sample was used as the reference.

Gas-phase spectra for each of the simulants were collected for reference using a Nicolet Nexus 470 FTIR spectrometer with a home-built high-pressure flow cell. For these measurements, nitrogen was passed through a glass bulb containing ~5 mL of simulant, which transported the simulant vapor into the flow cell. Each spectrum shown below represents the average of 256 scans collected at 4 cm^{-1} resolution with a 30 mm aperture and 1.89 cm/s scanner velocity.

Temperature-Programmed Desorption. An axial ionizer mass spectrometer (Extrel) was used to monitor the incident flux of gas during surface dosing and to measure the desorption rate for the TPD studies. Immediately following simulant dosing, the sample was annealed to ensure a uniform adsorbate distribution throughout the silica sample. As shown by Zubkov et al.,[35] who performed TPD of N_2 on highly porous surfaces, a uniform distribution of adsorbate is required for accurate interpretation of the resulting spectra. They demonstrated that a uniform distribution of adsorbates was evidenced by aligned high-temperature edges of TPD spectra recorded at different coverages, which indicates that the adsorbates are sufficiently mobile to migrate to the strongest adsorption sites. The sample annealing temperatures used in this work were 250 K for MDCP, 275 K for DMCP, and 300 K for TMP, DMMP, and DIMP.

To begin the TPD measurements with different initial coverages, the sample was annealed for different durations (between 1 s and 15 min). Immediately following annealing, the sample temperature was reduced to 195 K. Then, TPD measurements were conducted using a 0.2 K/s thermal ramp regulated with a proportional-integral-derivative controller (Honeywell) and custom power supply. This relatively slow ramp provided sufficient time for molecules to diffuse throughout the silica sample prior to desorbing.

Quantum Chemical Calculations. Quantum chemical calculations were performed to provide molecular insight into the bonding geometries and electronic structure of the organophosphorous compounds on silica.[50] Beyond the simulant molecules, calculations have also been performed on the agent sarin. Since the thermal treatment in the experiments renders a silica surface dominated by isolated silanol groups (i.e., the concentration of geminal and vicinal silanols is minimal), all of the computational efforts were directed at modeling isolated silanol groups with the highest accuracy possible. An isolated silanol molecule (H_3SiOH) represents the crudest possible model of the experimental surface groups and was employed in a subset of the calculations to ascertain whether the changes in the adsorption energies observed in the experiment apply to this simple model. This reduced-dimensionality surface model enabled the estimation of the adsorption energy using MP2 theory at the complete-basis-set (CBS) limit, which represents the highest-accuracy calculation on this type of system to date. To establish more quantitative comparisons with experiments, additional calculations were performed with a silica cluster of $Si_6O_8H_9$ stoichiometry, which is comparable to some of those used by Bermudez[7] and by Taylor et al. ($Si_4O_4H_1$, with dangling bonds capped by effective-core-potential F atoms) in their isolated-silanol calculations.[23]

With the H_3SiOH model, optimum geometries for the organophosphorous-silanol dimers were obtained using a combination of geometry optimizations at an affordable level of theory (MP2/6-31G*) with frozen scans and dual-level calculations at higher levels (MP2/cc-pVTZ and MP2/cc-pVQZ, respectively). From the 6-31G* calculations, frozen scans of the intermolecular distance between the two closest atoms of silanol and the organophosphorous species were performed at the MP2/cc-pVTZ level with a step size of 0.1 Å. Once the minimum was found in the MP2/cc-pVTZ intermolecular potential energy surface, a final calculation at the MP2/cc-pVQZ level was performed to further refine the energy. Use of a basis set as large as cc-pVQZ carried a significant computational overhead (for instance, the calculations involving the DIMP molecule interacting with a H_3SiOH molecule required 1353 basis functions) but has the benefit of affording a CBS limit estimate, which is unprecedented in prior studies of these systems. The frozen scans at the MP2/cc-pVTZ level showed that the MP2/6-31G* geometries were able to locate the minimum-energy Si−OH---O=P distance remarkably accurately. Geometry optimizations for the cluster calculations were performed at the B3LYP/6-31G* level, and dual-level calculations of the interaction energy were performed with those geometries at the MP2/cc-pVTZ and MP2/cc-pVQZ levels in some cases. The MP2/CBS energies were computed from the MP2/cc-pVTZ and MP2/cc-pVQZ energies using a two-point extrapolation formula.[36] All of the energy calculations removed the basis set superposition error employing the counterpoise method.

III. RESULTS

Characterization of Amorphous Silica. Immediately prior to each experiment, the silica sample was prepared by thermal annealing to 700 K for 5 min. Infrared spectra and X-ray photoelectron analysis revealed that this thermal treatment produced a surface that was nearly free from adsorbed water, had only trace hydrocarbon contamination, and contained a significant number of isolated SiO−H groups. The isolated hydroxyl groups are created during heating of silica as neighboring surface OH groups react to form water at elevated temperatures. The silanol surface density dependence on annealing temperature has been well characterized. For the preparation conditions employed here, we estimate the coverage of SiOH groups to be 2 silanols/nm^2.[29,30]

The infrared spectrum of the silica sample following thermal pretreatment is shown in Figure 2. The fundamental vibrational

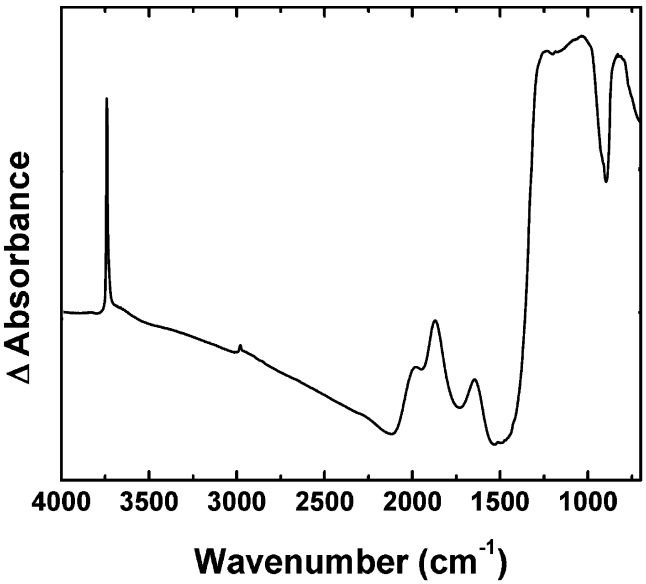

Figure 2. Transmission infrared spectrum of the silica sample at 225 K following pretreatment at 700 K for 5 min (see text).

mode of the isolated SiO−H groups appears as a narrow, intense peak at 3748 cm^{-1}. The small, broad shoulder on this peak at 3670 cm^{-1} is due to interstitial hydroxyl groups. These groups are also isolated hydroxyls; however, their location within pores between the packed silica particles significantly reduces their absorptivity and broadens their spectral response. The low-intensity peaks at 2998, 2959, 2933, and 2857 cm^{-1} are indicative of C−H stretches from a trace amount of hydrocarbon contamination within the silica sample. The three broad peaks at 1980, 1872, and 1648 cm^{-1} are due to overtones and combination modes of bulk silica. The most intense IR absorption that spans from 1300 to 1000 cm^{-1} is due to the asymmetric stretches of the bulk silica (the corresponding symmetric stretch is centered at 826 cm^{-1}).[33,34,37−39]

MDCP−Silica IR and TPD Data. We have explored the mechanisms of CWA simulant uptake by monitoring frequency changes in the original free SiO−H vibrational modes, during exposure of the particles to the simulant of interest, via infrared difference spectra. For the difference spectra, negative peaks represent vibrational modes that were originally present on the surface but changed in some way during adsorption, and positive features indicate the development of new or altered vibrational modes.

As discussed below, the spectral developments that occur upon exposure of clean silica to MDCP reveal that adsorption occurs almost exclusively through the formation of a phosphoryl−silanol hydrogen bond (Figure 3). The sharp

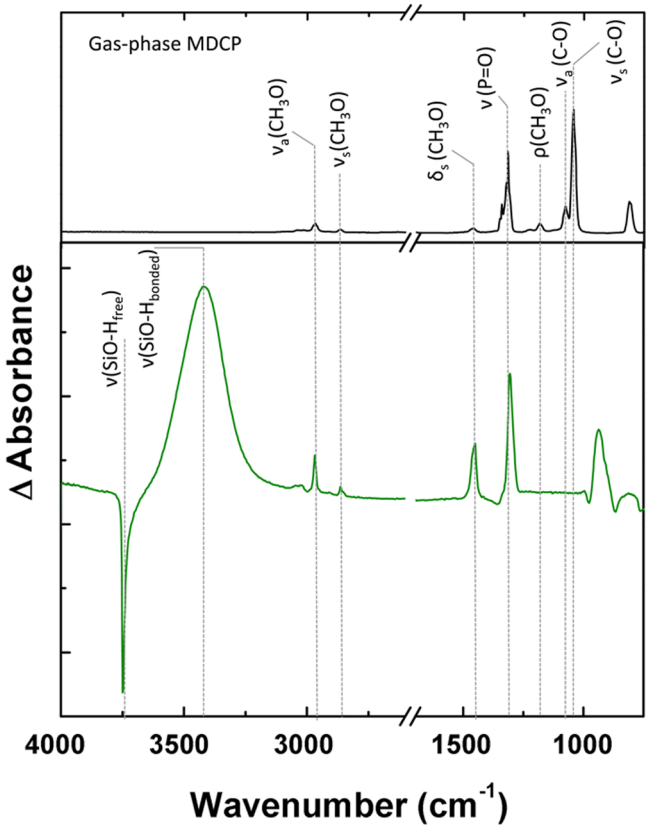

Figure 3. Infrared spectra of adsorbed MDCP on silica (lower spectrum) and gas-phase MDCP (top spectrum). Mode assignments are provided in Table 1.

negative feature at 3748 cm^{-1} appears as the originally isolated silanol groups establish new hydrogen bonds. These interactions shift the vibrational mode to lower frequencies and broaden the peak significantly. The relatively sharp features in the spectrum are due to the vibrational modes of the adsorbate. For reference, the vibrational spectrum of gas-phase MDCP is also provided in the figure. The assignments for each spectral feature are provided in Table 1.

Following infrared characterization of the vibrational modes for MDCP on silica, we employed TPD to determine the desorption energy and gain insight into the strength of the molecule−surface hydrogen-bonding interactions. The TPD distributions for several initial coverages of MDCP on silica are shown by the symbols in Figure 4A. For the TPD studies, the coverage is defined as the fraction of isolated SiOH groups that form a hydrogen-bonding complex with the adsorbate. This fraction is determined by the decrease in the intensity of the infrared absorbance for the isolated SiOH. For each TPD distribution, the molecules were dosed onto the surface held at T_s = 225 K. The simulant-covered surface sample was then heated to 250 K to remove weakly bound molecules and to create a uniform distribution of adsorbates throughout the sample.

dx.doi.org/10.1021/jp404265s | J. Phys. Chem. C 2013, 117, 15685−15697

Table 1. Assignments of the IR Peaks for MDCP in the Gas Phase and Adsorbed on Silica (See Ref 4)

	MDCP	
mode	gas	ads
$Si(O-H)_{free}$	*a*	3748
$Si(O-H)_{bonded}$	*a*	3421
$\nu_a(CH_3O)$	2967	2970
$\nu_s(CH_3O)$	2866	2859
$\delta_s(CH_3O)$	1452	1452
$\nu(P{=}O)$	1316	1304
$\rho(CH_3O)$	1184	*b*
$\nu_a(C-O)$	1077	*b*
$\nu_s(C-O)$	1044	*b*
$\nu(P-O-C)$	812	*b*

[a]Modes are not present in the molecule. [b]Modes are not observable in our sample due to strong overlap with bulk SiO_2 modes that block infrared transmission over this spectral range.

The TPD distributions at different coverages (determined following annealing) reveal that, as the coverage decreases, the maximum desorption rate shifts to higher temperatures and the high-temperature edges of the spectra coincide. As described in previous work, such characteristics in the TPD profiles indicate two important aspects of the system: (i) there is a distribution of sites with different binding energies and that (ii) the adsorbate is mobile enough at these temperatures to diffuse to the highest energy site prior to desorption. We also note that the mass spectrometric cracking pattern for MDCP molecules as they desorb from the surface is identical to that of the parent molecules, which indicates that molecular dissociation is very limited on the surface. This conclusion is supported by the IR data of Figure 3, which shows spectroscopic evidence for purely molecular adsorption.

Analysis of the TPD data was accomplished through inversion of the Polanyi–Wigner equation[12]

$$-\frac{d\Theta}{dt} = \nu e^{-E_d(\Theta)/k_B T_s}\Theta^n \quad (1)$$

where ν is the preexponential factor, Θ is coverage, T_s is the surface temperature, k_B is the Boltzmann constant, n is the order for desorption, and E_d is the activation energy for desorption.[35,40,41] Wilmsmeyer et al. recently demonstrated that this equation describes the desorption of CWA simulants from a packed sample of silica particles similar to that employed in the current study.[26] Alignment of the high-temperature sides of the variable-coverage TPD curves, as observed for each simulant studied here, indicates that the diffusion rate for these molecules, under our experimental conditions, is sufficient to ensure uniform coverage and that the rate-limiting step for desorption is the rupture of the adsorbate–surface bond.

The inversion analysis is accomplished by solving eq 1 for the desorption energy (for first-order desorption, $n = 1$).

$$E_d(\Theta) = -k_B T_s \ln\left(-\frac{d\Theta/dt}{\nu\Theta}\right) \quad (2)$$

Equation 2 provides the desorption energy, E_d, as a function of coverage by beginning with an assumed value for the preexponential factor, ν, for the highest coverage data in Figure 4A. The approximated $E_d(\theta)$ data is then numerically integrated to generate a series of simulated desorption profiles at the lower coverages used in the experiments. The preexponential is then treated as a variational parameter with the objective of minimizing the sum-of-squares of the residuals between the simulated TPD spectra and the experimental data.

The solid lines in Figure 4A are the simulated desorption curves for MDCP from the SiO_2 sample. The excellent fit of the data to the Polanyi–Wigner equation for first-order desorption suggests that this model accurately describes the desorption kinetics, which can be used to reveal the activation energy for desorption, $E_d(\theta)$, and the preexponential factor, ν. However, diffusion and readsorption can significantly affect TPD results.[42−47] For TPD studies of molecules from a particulate bed, the observed activation energy can correspond to that for desorption (when readsorption effects are negligible) or can correspond to the heat of adsorption (when readsorption effects dominate). For the case where adsorption is not an activated process, as is expected here, these values will be numerically equivalent, enabling accurate determination of the binding strength.[42−46] However, readsorption has a significant effect on the preexponential factor, which precludes a simple physical interpretation of this parameter.[42−46] The preexponential factor that provides the best fit to the TPD data shown in Figure 4 is $4.0 \times 10^{6\pm0.8}$ s^{-1}, which is a small value that reflects the fact that the molecules desorb and readsorb before reaching the outermost layer of particles in the packed sample

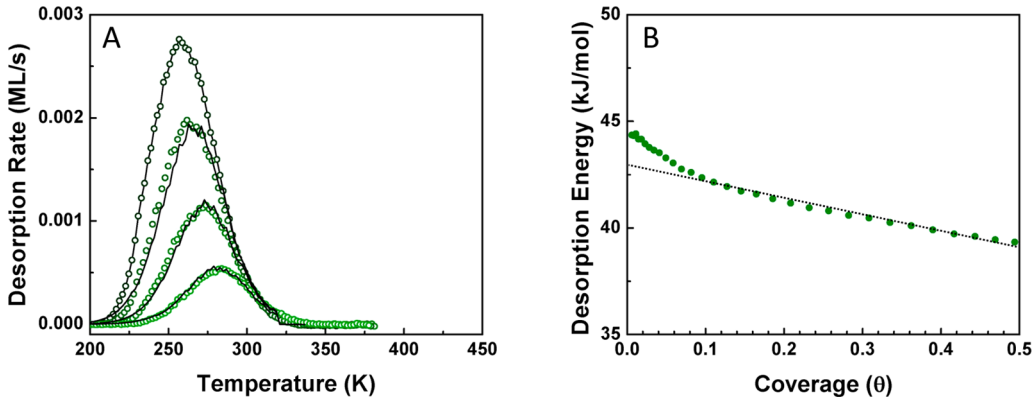

Figure 4. (A) Temperature-programed desorption of MDCP from amorphous silica particles. The circles are experimental data, and the lines are simulations based on the inversion analysis (see text for details). Following sample dosing, the molecules were desorbed at a heating rate of 0.2 K/s. The initial coverages were 0.11, 0.25, 0.34, and 0.50 ML. (B) Desorption energy vs MDCP coverage for the silica sample. The points were obtained by inversion of the 0.5 ML curve in panel A using the experimentally determined $\nu = 4 \times 10^6$ s^{-1} (see text for details).

dx.doi.org/10.1021/jp404265s | J. Phys. Chem. C 2013, 117, 15685−15697

and entering the vacuum.[44,45] Rather than discussing the entropic contributions to the desorption kinetics (information contained within the preexponential factor), the primary focus of this work is on the activation energy. The desorption energy distribution as a function of coverage ($E_d(\theta)$) is provided in Figure 4B, where the extrapolation to zero coverage yields a desorption energy of 43.0 ± 0.8 kJ/mol.

TMP−Silica IR and TPD Data. TMP appears to bind to silica much more strongly than the MDCP molecule described above. Figure 5 shows the IR difference spectrum of the silica sample following exposure of silica to TMP. The gas-phase spectrum of TMP is also provided as a reference, and the likely mode assignments are listed in Table 2. Compared with MDCP, the IR data reveal a much greater distortion of the SiO−H stretch as the peak vibrational frequency of this mode shifts by 558 cm^{-1}. The more dramatic shift suggests that the binding and desorption energy for TMP may be larger than for the dihalogen molecule.

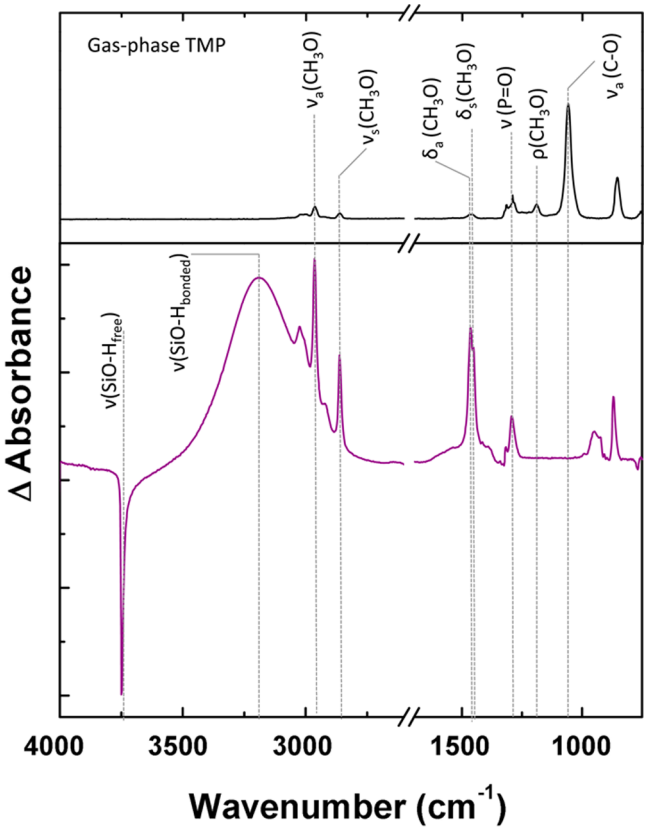

Figure 5. Infrared spectra of adsorbed TMP (bottom) on silica and gas-phase TMP (top). Mode assignments are provided in Table 2.

The desorption energy for TMP was measured in the same way as described above for MDCP, and the data are provided in Figure 6A. The excellent fit (solid line) of the simulated data to the actual experimental data provides confidence in the use of the inversion analysis to determine the desorption energy for this molecule. The $E_d(\theta)$ distribution is provided in Figure 6B. Although the overall shape of the curve is very similar to that of MDCP, the desorption energy in the limit of zero coverage is 52.4 ± 0.6 kJ/mol, which is 22% greater than the binding energy of MDCP. The differences between the simulants examined in this work will be elaborated upon in the Discussion section with the aid of results from the ab initio calculations.

Table 2. Assignments of the IR Peaks for TMP in the Gas Phase and Adsorbed on Silica (See Ref 4)

	TMP	
mode	gas	ads
$Si(O-H)_{free}$	*a*	3748
$Si(O-H)_{bonded}$	*a*	3190
$\nu_a(CH_3O)$	2964	2963
$\nu_s(CH_3O)$	2862	2862
$\delta_a(CH_3O)$	1465	1464
$\delta_s(CH_3O)$	1453	1454
ν(P═O)	1291	1274
ν_a(C−O)	1059	*b*
ν(P−O−C)	855	869

[a]Modes are not present in the molecule. [b]Modes are not observable in our sample due to strong overlap with bulk SiO_2 modes that block infrared transmission over this spectral range.

DIMP−Silica IR and TPD Data. The CWA sarin contains a methyl group, an isopropoxy group, and a halogen group around the central phosphoryl moiety. Therefore, DIMP was chosen as a simulant to investigate how bulky isopropyl groups influence uptake on the polar silica surface. Of the simulants explored in the current study, DIMP binds most readily and strongly to the surface of silica. Saturation of the sample by DIMP occurred following less than 100 langmuir of exposure, and the resulting infrared spectrum of the adsorbate exhibited a shift in the SiO−H mode of 660 cm^{-1}. This shift is evident in the IR difference spectrum of Figure 7. Assignments of the peaks in this spectrum are provided in Table 3.[48]

TPD measurements, shown in Figure 8A, together with the distribution of desorption energies as a function of coverage (Figure 8B), verify that DIMP interacts much more strongly with the silica surface than either MDCP or TMP. Overall, we find that the desorption energy for DIMP, in the limit of zero coverage, is 57.9 ± 1.0 kJ/mol, nearly 15 kJ/mol higher than MDCP. The role of the isopropoxy groups in enhancing the molecule−surface interaction energy may be through dispersion forces or by affecting the electron density on the oxygen atom involved in hydrogen bonding. These effects have been explored in detail using electronic structure calculations, presented within the context of the following discussion.

IV. DISCUSSION

Infrared spectroscopic and temperature-programmed desorption studies provide insight into the binding mechanism and strength of CWA simulant interactions on particulate silica. The native surface of amorphous silica is typically hydrophilic due to the presence of stable hydroxyl groups. These silanol groups serve as strong binding sites for many types of polar gases through dipole−dipole type interactions. In this study, we focus on the hydrogen-bonding forces between the silanol groups and hydrogen-bond-acceptor groups on CWA simulant molecules. Infrared spectroscopic measurements are excellent probes of these interactions because hydrogen bonding at the gas−surface interface is often accompanied by changes in the vibrational frequency of molecular motions that are involved in the hydrogen bond. In addition to IR studies, TPD measurements and electronic structure calculations were employed to determine the strength of the molecule−surface interactions.

dx.doi.org/10.1021/jp404265s | J. Phys. Chem. C 2013, 117, 15685−15697

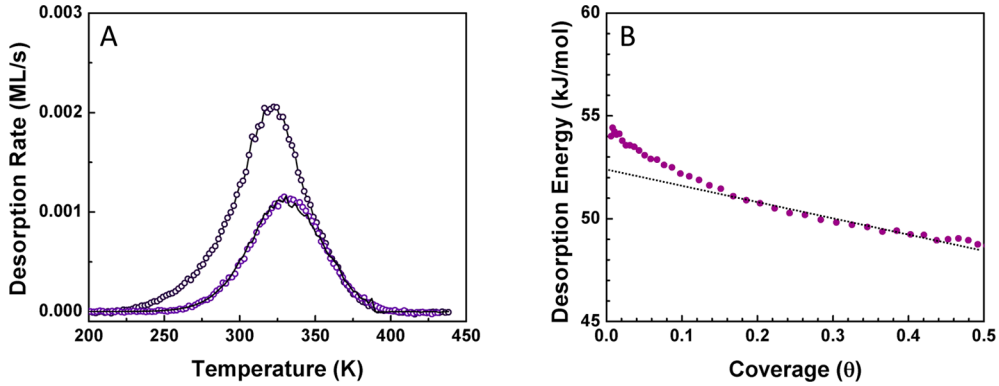

Figure 6. (A) Temperature-programed desorption of TMP from amorphous silica particles. The circles are experimental data, and the lines are simulations based on the inversion analysis (see text for details). Following sample dosing, the molecules were desorbed at a heating rate of 0.2 K/s. The initial coverages were 0.25 and 0.50 ML. (B) Desorption energy vs TMP coverage for the silica sample.

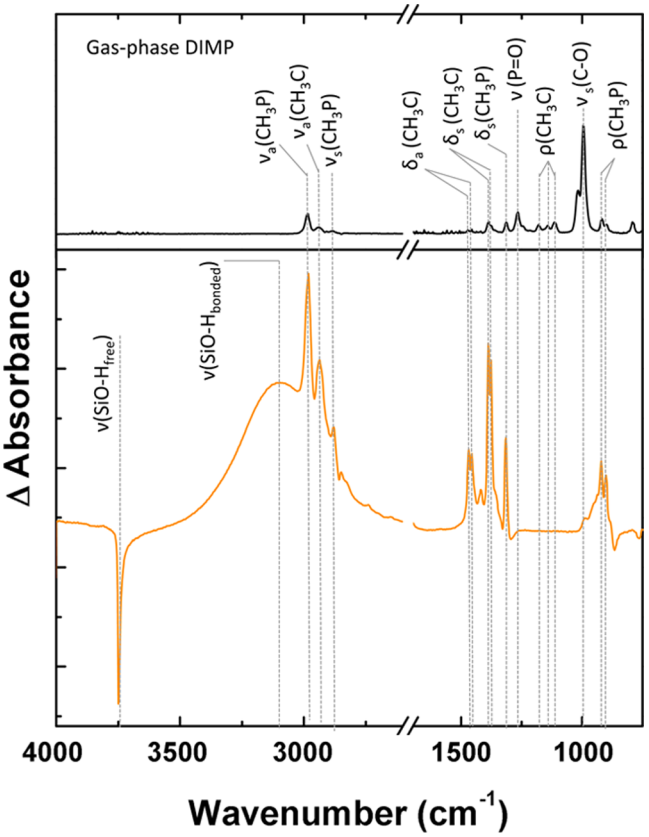

Figure 7. Infrared spectra of adsorbed DIMP (bottom) on silica and gas-phase DIMP (top). Mode assignments are provided in Table 3.

Table 3. Assignments of the IR Peaks for DIMP in in the Gas Phase and Adsorbed on Silica (See Ref 48 for Mode Assignments)

	DIMP	
mode	gas	ads
$Si(O-H)_{free}$	*a*	3748
$Si(O-H)_{bonded}$	*a*	3089
$\nu_a(CH_3P)$	2985	2982
$\nu_a(CH_3C)$	2940	2937
$\nu_s(CH_3P)$	2883	2880
$\delta_a(CH_3C)$	1473	1470
$\delta_a(CH_3C)$	1457	1457
$\delta_s(CH_3C)$	1387	1388
$\delta_s(CH_3C)$	1377	1377
$\delta_s(CH_3P)$	1314	1316
$\nu(P{=}O)$	1266	*b*
$\rho(CH_3C)$	1180	*b*
$\rho(CH_3C)$	1143	*b*
$\rho(CH_3C)$	1113	*b*
$\nu_a(C-O)$	1017	*b*
$\nu_s(C-O)$	995	*b*
$\rho(CH_3P)$	918	921
$\rho(CH_3P)$	900	902

[a]Modes are not present in the molecule. [b]Modes are not observable in our sample due to strong overlap with bulk SiO_2 modes that block infrared transmission over this spectral range.

Adsorption Mechanism. The infrared spectral signature for hydrogen-bond formation between isolated surface hydroxyl groups and adsorbates is the emergence of a broad SiO−H stretching mode. In addition, this mode is typically red-shifted from the frequency of the isolated OH stretch due to the redistribution of charge from the SiO−H bond to the SiOH---OR hydrogen bond. These changes are clearly evident in Figures 3, 5, and 7 for the binding of the OP simulants to silica. While the spectral changes in the surface SiO−H mode clearly reveal that this surface hydroxyl group serves as the hydrogen-bond donor site, there are multiple groups within the simulants that may serve as hydrogen-bond acceptor sites. In particular, hydrogen bonding may occur through interactions of the lone-pair of electrons on the sp^2 or the sp^3 oxygen atoms present on all simulants. In addition, MDCP contains two chlorine atoms that may also serve as hydrogen-bond acceptor sites. Because hydrogen-bonding interactions redistribute charge within the functional group involved, one may expect that differences between gas-phase spectra and the surface adsorbates may reveal the most likely sites for hydrogen bonding to occur. Tables 1, 2, and 3 directly compare the vibrational frequencies of the gas-phase species to the surface-adsorbed simulants. The vibrational frequencies of the gas-phase and surface-bound molecules are remarkably similar. The differences are within ~5 cm^{-1} of each other. The only exception is the large shift observed for the P═O mode in MDCP and TMP, suggesting that uptake is governed by hydrogen bonding through the sp^2 oxygen atom. Unfortunately, the frequency of the P═O mode for adsorbed DIMP and DMMP (see below) is obscured by the strong absorbance of the silica and cannot be observed.

dx.doi.org/10.1021/jp404265s | J. Phys. Chem. C 2013, 117, 15685−15697

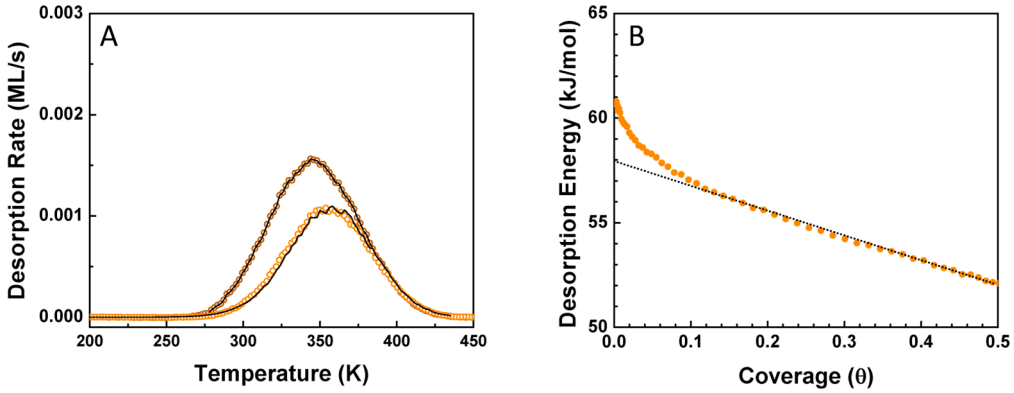

Figure 8. (A) Temperature-programed desorption of DIMP from amorphous silica particles. The circles are experimental data, and the lines are simulations based on the inversion analysis (see text for details). Following sample dosing, the molecules were desorbed at a heating rate of 0.2 K/s. The initial coverages were 0.37 and 0.50 ML. (B) Desorption energy vs DIMP coverage for the silica sample.

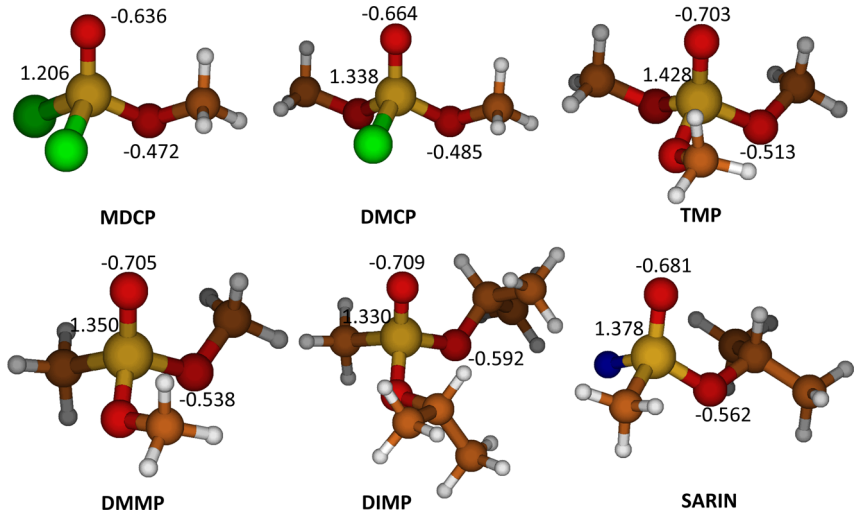

Figure 9. Minimum-energy structures (MP2/6-31G*) and Mulliken charges on P and O atoms (MP2/cc-pVQZ//6-31G*) of the organophosphorous compounds considered in this work: red = O, gold = P and Si, brown = C, white = H, green = Cl, and blue = F.

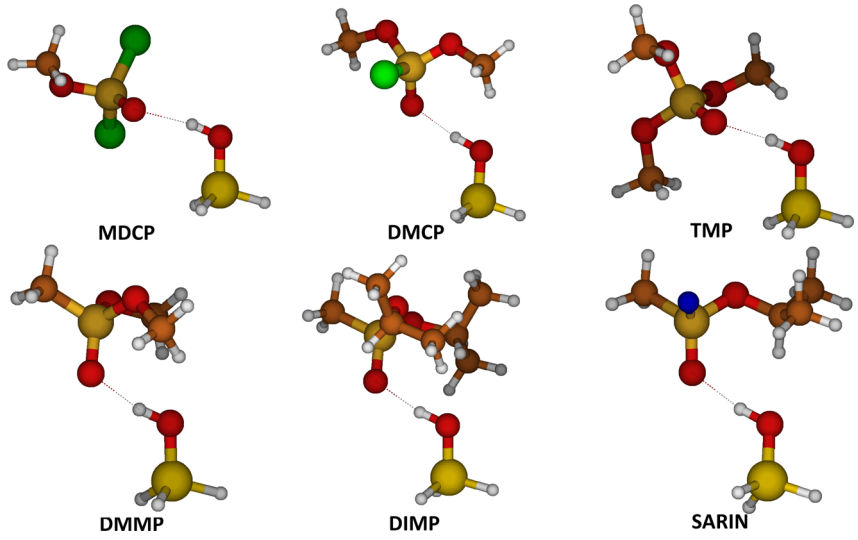

Figure 10. Minimum-energy structures of organophosphorous compounds interacting with silanol: red = O, gold = P, brown = C, white = H, green = Cl, and blue = F.

However, electronic structure calculations support the assertion that binding for all three molecules does indeed occur preferentially through SiO−H---O═P interactions. To further explore which of the hydrogen-bond-accepting groups on the adsorbates binds to the silanol sites on silica, electronic structure calculations were performed.[50] Figure 9 shows MP2/

dx.doi.org/10.1021/jp404265s | J. Phys. Chem. C 2013, 117, 15685−15697

Table 4. Calculated and Measured Interaction Energies between OP Compounds and a Silanol Gas-Phase Molecule[a]

molecule	O atom charge[b]	MP2/cc-pVTZ[c]	MP2/cc-pVQZ	MP2/CBS	exp (E_d)
MDCP	−0.636	24.92 (33.30)	27.21 (35.98)	28.88 (37.94)	43.0 ± 0.8
DMCP	−0.664	33.19 (37.53)	35.91	37.89	48.4 ± 1.0
TMP	−0.703	37.77 (44.21)	40.59	42.64	52.4 ± 0.6
DMMP	−0.705	39.87 (45.82)	42.55	44.50	54.5 ± 0.3
DIMP	−0.709	44.11 (51.86)	47.56	50.08	57.9 ± 1.0
sarin	−0.681	37.22 (41.51)	38.89	43.56	

[a]The experiments correspond to activation energies for desorption from a silica surface measured in temperature-programmed desorption and the calculations to the difference in electronic energy between the interaction complex and separated reagents. [b]MP2/cc-pVQZ. [c]Values between parentheses correspond to the interaction energy between the OP compounds and a silica cluster (see text).

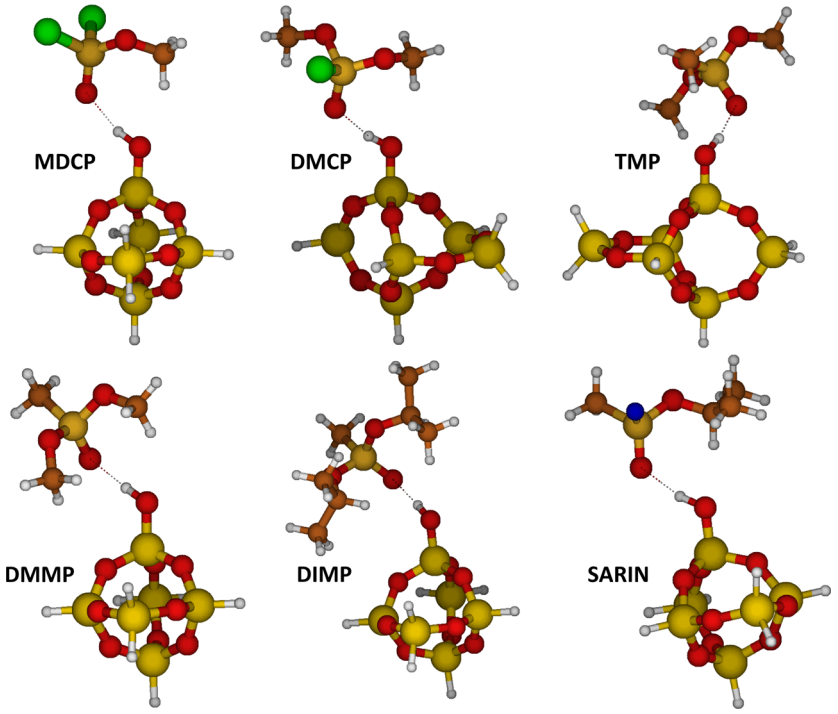

Figure 11. Minimum-energy structures of organophosphorous compounds interacting with an isolated silanol group on a silica cluster: red = O, gold = P and Si, brown = C, white = H, green = Cl, and blue = F.

cc-pVQZ Mulliken charges on optimized structures of the adsorbates. Clearly, the electronic density around the oxygen atom with formal sp^2 hybridization is larger than around the oxygen atoms of the methoxy or isopropoxy moieties bound to the phosphorus atom (sp^3 hybridization). These results suggest that hydrogen bonding to silanol groups via the phosphoryl group should be stronger than via the rest of oxygen atoms in the adsorbates. To verify this expectation, minimum-energy structures of the interaction of all six OP species in Figure 9 with silanol were determined. The results are depicted in Figure 10. In all cases, the calculations indicate that Si−O−H---O═P binding is significantly stronger than binding to the sp^3 oxygen atoms of the alkoxy groups. For instance, at the MP2/CBS level, the dimer involving MDCP shown in Figure 10 is about 10 kJ/mol stronger than the complex involving binding to the oxygen atom in the methoxy moiety (28.9 vs 18.5 kJ/mol binding energies, respectively). For the rest of the dimers, the difference between the adsorption energy when the hydrogen bond acceptor is the sp^2 or sp^3 oxygen atoms is even larger. For instance, in TMP, the difference raises to 14.3 kJ/mol (42.6 vs 28.3 kJ/mol). Additional calculations were conducted to locate energy minima in which the silanol group interacts directly with the Cl atoms in MDCP and DMCP, but all geometry optimizations led to either one of the minima involving a Si−O−H----O interaction instead, indicating that hydrogen bonding through the halogen atoms in the OP species is not as stabilizing as through the oxygen atoms.[50]

Desorption Energy. As described in the Results section, we have experimentally measured the activation energy for desorption for these three molecules through variable coverage TPD measurements followed by an inversion analysis to determine the preexponential factor. The coverage-dependent desorption energies for each simulant are provided in Figures 4B, 6B, and 8B.

The inversion analysis reveals a monotonic increase in $E_d(\theta)$ as coverage decreases for all three simulants. The same trend was recently reported for the related simulants, DMMP and DMCP (see Figure 1),[26] suggesting that the effect is general for the desorption of OPs from particulate amorphous silica. The increase in energy reveals that there are a variety of surface binding sites or configurations, each leading to a slightly different energy. Alternatively, there may be small repulsive interactions between the adsorbates, the extent of which depends on coverage. The distribution in desorption energy

dx.doi.org/10.1021/jp404265s | J. Phys. Chem. C 2013, 117, 15685−15697

spans approximately 5 kJ/mol for each simulant over the surface coverage regime of θ = 0.05−0.5 monolayers. Interestingly, the desorption energy for every simulant increases abruptly by several kJ/mol near zero coverage. The reason for this increase in energy is likely due to the fact that the molecules residing on the surface at the highest temperatures (where the coverage is lowest) bind to the highest energy sites. We estimate that these high-energy binding sites account for approximately 5% of the first monolayer on the surface. The sites are likely high-energy defects consisting of multiple silanol groups in close proximity. Previous work has shown that the strongest binding sites for polar molecules on silica occur at geminal and vicinal silanols, where multiple hydrogen-bonding interactions occur. Adsorption energies for DMMP on silica may be over 100 kJ/mol when the P═O group can form dual hydrogen bonds with adjacent surface OH groups.[7,23]

One of the primary goals of the current work is to assess the hydrogen-bonding energy to a single isolated surface silanol group. The desorption energy for an isolated molecule from a single silanol can be estimated from the $E_d(\theta)$ distribution curves by extrapolating the linear region of the desorption energy curve (dashed line in Figures 4B, 6B, and 8B) to zero coverage. As indicated in the figures, the extrapolated values are 43.0 ± 0.8, 52.4 ± 0.6, and 57.9 ± 1.0 kJ/mol for MDCP, TMP, and DIMP, respectively. The calculations involving binding of the CWA simulants to a silanol molecule through the sp^2 oxygen atom reveal exactly the same trend, with MP2/CBS values of 28.9, 42.6, and 50.1 kJ/mol for the same molecules. While the absolute difference between the calculated and measured energies is relatively large, an important result is that the relative deviation between the calculations and measurement is constant. This can be further corroborated in Table 4, where the results for all five mimics are shown, and a relatively constant difference between experiment and theory of about 10 kJ/mol can be appreciated. The presence of a constant difference between theory and experiment in this study is in contrast to recent work[23] where the differences between theory and experiment were more erratic. Another note of importance is that the simulations consistently underestimate the measurements. Taken together, these observations suggest that a model as crude as a single gas-phase silanol molecule captures the fundamental aspects of the interactions with a silica surface in the experiment and that, as expected, the experimental surface is dominated by isolated silanol groups.

The nature of the surface used in this study (dominated by isolated silanol groups), together with the use of the UHV environment, provides an excellent opportunity to benchmark theoretical methods that transcend a single gas-phase silanol molecule and attempt to model the silica surface more realistically. To this end, we have constructed a silica cluster with an isolated silanol group of dimensions comparable to those utilized in prior studies.[7] Figure 11 shows minimum-energy structures of such cluster interacting with the OP compounds investigated in this work, and MP2/cc-pVTZ energies are listed in Table 4. Comparison of the interaction energies for the mimics reveals the same trend measured in the experiment and anticipated by the gas-phase silanol calculations. In addition, comparison of the MP2/cc-pVTZ energies for both the gas-phase silanol molecule and the silica cluster shows that the silica results match experiments more closely than the simple gas-phase silanol calculations. In fact, the underestimation of the experiment by the MP2/cc-pVTZ cluster calculations is reduced to 7−9 kJ/mol. Moreover, because, as seen in the gas-phase H_3SiOH---OP calculations, use of a correlation-consistent basis set provides larger binding energies with use of increasing cardinal number, one can expect that MP2/cc-pVQZ and MP2/CBS calculations will match experiment even more accurately. To prove this point, we have performed such calculations for the least computationally expensive mimic of the series, MDCP. We note that 3 of the 5 energies required to obtain the counterpoise-corrected MP2/cc-pVQZ energy involved as many as 1521 basis functions. The resulting MP2/CBS energy (37.94 kJ/mol) underestimates experiment by less than 5 kJ/mol and lends further confidence to the computational approach utilized in this work and the conclusions drawn from it. A caveat in the theory/experiment comparison in Table 4 is that while the calculations correspond to the difference in electronic energy between separated species and the minimum-energy complex, the measurements correspond to activation energies of desorption at the desorption temperature. A truly quantitative comparison between theory and experiment requires the inclusion of zero-point energies to the electronic energies, the addition of vibrational, rotational, and translational thermal corrections, transformation of the internal energy to enthalpy, and transformation of enthalpy to activation energy of desorption. For MDCP, all these corrections make the calculated activation energy of desorption ∼3.4 kJ/mol larger than the binding energy in Table 4, bringing agreement between theory and experiment even closer. Given the observed convergence between the experimentally measured desorption energies and the calculated energies for the test case of MDCP (when the proper transformations are included), we expect that the theoretical and experimental energies will agree to within the 4 kJ/mol (∼1 kcal/mol) once MP2/CBS extrapolations become feasible for all of the simulants used in this work.

For the five CWA simulants studied by both experimental and theoretical methods, binding to silica appears to occur through the sp^2 oxygen atom of the OP. However, the strengths of the adsorbate−surface bonds depend on structure. The activation energies for desorption measured in the experiment follow the trend MDCP < DMCP < TMP < DMMP < DIMP. This trend is exactly reproduced by the calculations and demonstrates the critical role of substituents in governing the adsorption energies through hydrogen-bonding interactions. The electronic structure calculations described above indicate that the experimentally measured desorption energy from an isolated silanol group is directly related to the charge on the sp^2 oxygen atom of the simulant. This trend is revealed in Figure 12, which shows the atomic charge on the sp^2 oxygen plotted against the experimentally measured desorption energy for each simulant. This near linear correlation further supports that the dominant interaction pathway is through the P═O oxygen atom for every simulant studied. In addition, the results reveal that the chlorine substituents do not serve as hydrogen-bond acceptor sites nor do they interact strongly with the surface in other ways. The net effect of the halogen atoms appears to be that of withdrawing electron density from the sp^2 oxygen, which is the most important factor in determining the strength of adsorption and the activation energy for desorption.

Badger−Bauer Relationship: IR Frequency and Desorption Energy Correlation. Badger and Bauer were among the first to show that the stretching frequency for hydrogen-bonded hydroxyl groups in binary solutions is directly proportional to the strength of the solvent−solute interactions.[49] However, there are few examples of this relationship

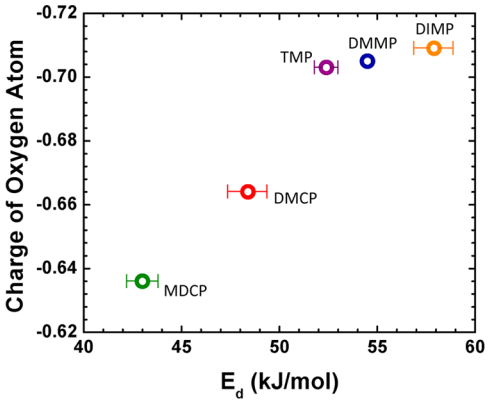

Figure 12. Calculated charge on the sp^2 oxygen atom of the simulant versus the experimentally determined desorption energy from TPD measurements.

at the gas–surface interface, where solvation is absent. In an effort to reveal the surface analogue to the Badger–Bauer relationship, we have compiled the infrared and desorption data for the five CWA simulants studied with the inversion analysis described above (Figures 13A,B). From these sets of data, we constructed a Badger–Bauer type plot for surface binding (Figure 13C).

Clearly, the Badger–Bauer relationship holds over a range of desorption energies and molecular structures. The shift in SiO–H vibration energy to lower wavenumber is due to the charge redistribution within the hydroxyl bond as the hydrogen interacts with the adsorbate. These hydrogen-bond donor type interactions weaken the original SiO–H bond leading to greater anharmonicity in the stretching mode of silanol OH and lower energy vibrational transitions. Therefore, it is not surprising that there is a correlation between desorption energy and frequency; however, we must point out that the relationship is remarkably linear.

Predicting the Sarin-Silica Desorption Energy. The strong charge–E_d correlation suggests that the binding energy for the actual CWAs to surface silanol groups is determined nearly exclusively by the charge on the sp^2 oxygen atom of the molecule and that this information may help predict the actual desorption energy for the agents from amorphous silica. For example, the isopropyl substituent on the agent sarin (see Figure 1) will have the effect of donating charge to the sp^2 oxygen, thereby increasing the adsorption energy, as observed for DIMP relative to DMMP. However, this effect will likely be balanced by the significant electron-withdrawing character of the fluorine group, which should serve to lower the desorption energy (as observed for DMCP and MDCP).

Our electronic structure calculations for sarin indicate that the charge on the sp^2 oxygen atom of this molecule (MP2/cc-pVQZ) is −0.681. By using the plot of Figure 12 as a standard calibration curve, we predict that the actual desorption energy for sarin from amorphous silica composed primarily of isolated silanol groups is ∼50 kJ/mol.

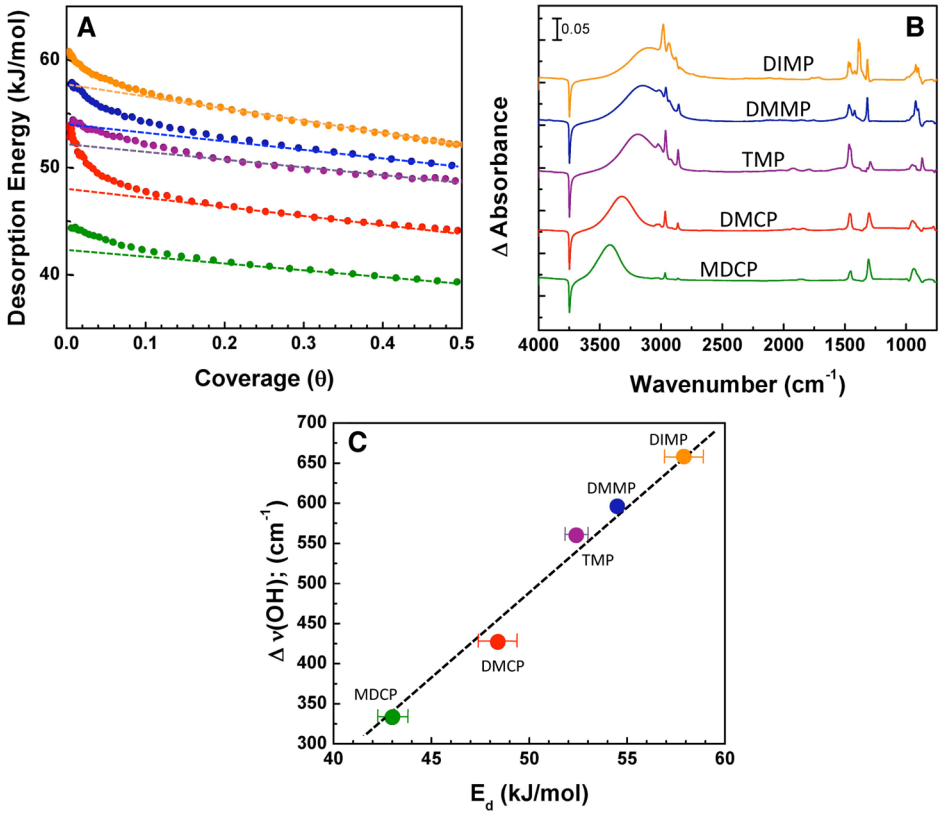

Figure 13. (A) $E_d(\theta)$ curves for the desorption of five CWA simulants from partially hydroxylated silica, (B) compilation of the FTIR spectra for each simulant adsorbed to silica at a coverage of 0.5 mL, and (C) the change in peak frequency for the SiO–H surface vibration mode as a function of desorption energy for all five simulants. Consistent with the colors used in the previous figures, the points and spectra shown in green are for the simulant MDCP, red are for DMCP, purple are for TMP, blue are for DMMP, and orange are for DIMP.

dx.doi.org/10.1021/jp404265s | J. Phys. Chem. C 2013, 117, 15685–15697

V. SUMMARY

The adsorption of organophosphorous compounds on an amorphous silica surface has been investigated using IR spectroscopy, TPD, and ab initio calculations. The results suggest that hydrogen-bonding interactions occur between surface silanol groups and the adsorbates, with the sp^2 oxygen atom of the adsorbates' phosphoryl group acting as the primary hydrogen-bond acceptor. The chemical nature of the substituent groups on the phosphoryl group of the OP adsorbates modulates the strength of the interaction with the silanol groups on the surface, and this is revealed by the magnitude of the shift of the surface SiO−H stretching frequencies, the values of the measured desorption energy, and the calculated binding energy. All of the results indicate that the strength of the interaction of CWA simulants with silica follows the MDCP < DMCP < TMP < DMMP < DIMP trend.

Remarkably, the results of the IR and TPD experiments and QC calculations can all be explained by the universal trend in electron-withdrawing capacity via the inductive effect of substituent groups (−halogens > −OR > −R) around the phosphorus atom of the OP species studied in this work, which is further corroborated by an analysis of atomic charges. MDCP contains two −Cl and one −OR substituent, and its binding to silica is weaker than DMCP, which contains one −Cl and two −OR substituents. TMP has three −OR substituents, and the decrease in electron-withdrawing capacity with respect to DMCP leads to a higher binding energy. DMMP replaces one of the −OR substituents with an −R substituent, which is not as electron withdrawing, further increasing the binding energy. DMMP and DIMP have the same type of substituents around the phosphorus atom, but the higher electron density of the isopropyl moiety diminishes the electron-withdrawing ability of the −OR groups in DIMP, yielding a larger binding energy than DMMP.

These studies demonstrate that the hydrogen-bonding energy for the actual agents is likely very high, as has been suggested in recent work closely related to the studies presented here.[7,23] Together, these experimental measurements and theoretical calculations are providing new insight into the mechanisms and strength of hydrogen bonding between CWAs and surfaces. These types of molecule−surface hydrogen-bonding interactions play a major role in determining their uptake into important sorbent materials, filters, and coatings that contain hydrogen-bond donor groups.

AUTHOR INFORMATION

Corresponding Author

*E-mail jrmorris@vt.edu (J.R.M.).

Notes

The authors declare no competing financial interest.

ACKNOWLEDGMENTS

The support of the Army Research Office, W911NF-09-1-0150, the Defense Threat Reduction Agency, W911NF-06-1-0111, and the National Science Foundation CHE-0547543 is gratefully acknowledged. The authors also acknowledge Advanced Research Computing at Virginia Tech for providing computational resources and technical support that have contributed to the results reported within this paper.

REFERENCES

(1) Kim, K.; Tsay, O. G.; Atwood, D. A.; Churchill, D. G. Destruction and Detection of Chemical Warfare Agents. *Chem. Rev.* **2011**, *111*, 5345−5403.

(2) Barr, T. L. ESCA Study of Termination of Passivation of Elemental Metals. *J. Phys. Chem.* **1978**, *82* (16), 1801−1810.

(3) Kanan, S. M.; Lu, Z. X.; Tripp, C. P. A Comparative Study of the Adsorption of Chloro- and Non-Chloro-Containing Organophosphorus Compounds on WO_3. *J. Phys. Chem. B* **2002**, *106* (37), 9576−9580.

(4) Kanan, S. M.; Tripp, C. P. An Infrared Study of Adsorbed Organophosphonates on Silica: A Prefiltering Strategy for the Detection of Nerve Agents on Metal Oxide Sensors. *Langmuir* **2001**, *17* (7), 2213−2218.

(5) Ferguson-McPherson, M. K.; Low, E. R.; Esker, A. R.; Morris, J. R. Sorption of Dimethyl Methylphosphonate within Langmuir-Blodgett Films of Trisilanolphenyl Polyhedral Oligomeric Silsesquioxane. *J. Phys. Chem. B* **2005**, *109* (40), 18914−18920.

(6) Ferguson-McPherson, M. K.; Low, E. R.; Esker, A. R.; Morris, J. R. Corner Capping of Silsesquioxane Cages by Chemical Warfare Agent Simulants. *Langmuir* **2005**, *21* (24), 11226−11231.

(7) Bermudez, V. M. Computational Study of the Adsorption of Trichlorophosphate, Dimethy Methylphosphonate, and Sarin on Amorphous SiO_2. *J. Phys. Chem. C* **2007**, *111*, 9314−9323.

(8) Bermudez, V. M. Quantum-Chemical Study of the Adsorption of DMMP and Sarin on Gamma-Al_2O_3. *J. Phys. Chem. C* **2007**, *111* (9), 3719−3728.

(9) Bermudez, V. M. Energy-Level Alignment in the Adsorption of Phosphonyl Reagents on Gamma-Al_2O_3. *Surf. Sci.* **2008**, *602* (11), 1938−1947.

(10) Bermudez, V. M. Computational Study of Environmental Effects in the Adsorption of DMMP, Sarin, and VX on Gamma- Al_2O_3: Photolysis and Surface Hydroxylation. *J. Phys. Chem. C* **2009**, *113* (5), 1917−1930.

(11) Bermudez, V. M. Effect of Humidity on the Interaction of Dimethyl Methylphosphonate (DMMP) Vapor with SiO_2 and Al_2O_3 Surfaces, Studied Using Infrared Attenuated Total Reflection Spectroscopy. *Langmuir* **2010**, *26* (23), 18144−18154.

(12) Polanyi, M.; Wigner, E. Über Die Interferenz Von Eigenschwingungen Als Ursache Von Energieschwankungen Und Chemischer Umsetzungen. *Z. Phys. Chem., Abt A* **1924**, *139*, 439−452.

(13) Gay, I. D.; McFarlan, A. J.; Morrow, B. A. Trimethyl Phosphite Adsorbed on Silica - An NMR and Infrared Study. *J. Phys. Chem.* **1991**, *95* (3), 1360−1368.

(14) Gordon, W. O.; Tissue, B. M.; Morris, J. R. Adsorption and Decomposition of Dimethyl Methylphosphonate on Y_2O_3 Nanoparticles. *J. Phys. Chem. C* **2007**, *111* (8), 3233−3240.

(15) Ekerdt, J. G.; Klabunde, K. J.; Shapley, J. R.; White, J. M.; Yates, J. T. Surface-Chemistry of Organo-Phosphorus Compounds. *J. Phys. Chem.* **1988**, *92* (22), 6182−6188.

(16) Knagge, K.; Johnson, M.; Grassian, V. H.; Larsen, S. C. Adsorption and Thermal Reaction of DMMP in Nanocrystalline NaY. *Langmuir* **2006**, *22* (26), 11077−11084.

(17) Michalkova, A.; Gorb, L.; Ilchenko, M.; Zhikol, O. A.; Shishkin, O. V.; Leszczynski, J. Adsorption of Sarin and Soman on Dickite: An ab Initio ONIOM Study. *J. Phys. Chem. B* **2004**, *108* (6), 1918−1930.

(18) Michalkova, A.; Ilchenko, M.; Gorb, L.; Leszczynski, J. Theoretical Study of the Adsorption and Decomposition of Sarin on Magnesium Oxide. *J. Phys. Chem. B* **2004**, *108* (17), 5294−5303.

(19) Moss, J. A.; Szczepankiewicz, S. H.; Park, E.; Hoffmann, M. R. Adsorption and Photodegradation of Dimethyl Methylphosphonate Vapor at TiO_2 Surfaces. *J. Phys. Chem. B* **2005**, *109* (42), 19779−19785.

(20) Panayotov, D.; Kondratyuk, P.; Yates, J. T. Photooxidation of a Mustard Gas Simulant over TiO_2-SiO_2 Mixed-Oxide Photocatalyst: Site Poisoning by Oxidation Products and Reactivation. *Langmuir* **2004**, *20* (9), 3674−3678.

(21) Panayotov, D. A.; Morris, J. R. Catalytic Degradation of a Chemical Warfare Agent Simulant: Reaction Mechanisms on TiO_2-

Supported Au Nanoparticles. *J. Phys. Chem. C* **2008**, *112* (19), 7496−7502.
(22) Panayotov, D. A.; Morris, J. R. Uptake of a Chemical Warfare Agent Simulant (DMMP) on TiO_2: Reactive Adsorption and Active Site Poisoning. *Langmuir* **2009**, *25* (6), 3652−3658.
(23) Taylor, D. E.; Runge, K.; Cory, M. G.; Burns, D. S.; Vasey, J. L.; Hearn, J. D.; Griffith, K.; Henley, M. V. Surface Binding of Organophosphates on Silica: Comparing Experiment and Theory. *J. Phys. Chem. C* **2013**, *117* (6), 2699−2708.
(24) Taylor, D. E.; Runge, K.; Cory, M. G.; Burns, D. S.; Vasey, J. L.; Hearn, J. D.; Henley, M. V. Binding of Small Molecules to a Silica Surface: Comparing Experimental and Theoretical Results. *J. Phys. Chem. C* **2011**, *115* (50), 24734−24742.
(25) Vaiss, V. S.; Borges, I.; Leitao, A. A. Sarin Degradation Using Brucite. *J. Phys. Chem. C* **2011**, *115* (50), 24937−24944.
(26) Wilmsmeyer, A. R.; Uzarski, J.; Barrie, P. J.; Morris, J. R. Interactions and Binding Energies of Dimethyl Methylphosphonate and Dimethyl Chlorophosphate with Amorphous Silica. *Langmuir* **2012**, *28* (30), 10962−7.
(27) Henderson, M. A.; Jin, T.; White, J. M. A TPD/AES Study of the Interaction of Dimethyl Methylphosphonate with Alpha-Fe_2O_3 and SiO_2. *J. Phys. Chem.* **1986**, *90* (19), 4607−4611.
(28) Quenneville, J.; Taylor, R. S.; van Duin, A. C. T. Reactive Molecular Dynamics Studies of DMMP Adsorption and Reactivity on Amorphous Silica Surfaces. *J. Phys. Chem. C* **2010**, *114* (44), 18894−18902.
(29) Zhuravlev, L. T. Concentration of Hydroxyl-Groups on the Surface of Amorphous Silicas. *Langmuir* **1987**, *3* (3), 316−318.
(30) Zhuravlev, L. T. The Surface Chemistry of Amorphous Silica. Zhuravlev Model. *Colloids Surf., A* **2000**, *173* (1−3), 1−38.
(31) Kanan, S. M.; Tripp, C. P. Prefiltering Strategies for Metal Oxide Based Sensors: The Use of Chemical Displacers to Selectively Dislodge Adsorbed Organophosphonates from Silica Surfaces. *Langmuir* **2002**, *18* (3), 722−728.
(32) Nadler, M. P.; Nissan, R. A.; Hollins, R. A. FT-IR and FT-NMR Study of Organophosphorus Surface Reactions. *Appl. Spectrosc.* **1988**, *42* (4), 634−642.
(33) *Colloidal Silica: Fundamentals and Applications*; CRC Press: New York, 2006; Vol. *131*.
(34) *The Surface Properties of Silicas*; John Wiley & Sons: New York, 1998.
(35) Zubkov, T.; Smith, R. S.; Engstrom, T. R.; Kay, B. D. Adsorption, Desorption, and Diffusion of Nitrogen in a Model Nanoporous Material. II. Diffusion Limited Kinetics in Amorphous Solid Water. *J. Chem. Phys.* **2007**, *127* (18), 184708.
(36) Halkier, A.; Helgaker, T.; Jørgensen, P.; Klopper, W.; Koch, H.; Olsen, J.; Wilson, A. K. Basis-Set Convergence in Correlated Calculations on Ne, N_2, and H_2O. *Chem. Phys. Lett.* **1998**, *286* (3−4), 243−252.
(37) Buccuzzi, F.; Coluccia, S.; Ghiotti, G.; Morterra, C.; Zecchina, A. IR Study of Surface Modes on Silica. *J. Phys. Chem.* **1978**, *82* (11), 1298−1303.
(38) Tripp, C. P.; Hair, M. L. Reaction of Chloromethylsilanes with Silica: A Low-Frequency Infrared Study. *Langmuir* **1991**, *7*, 923−927.
(39) *Adsorption on Silica Surfaces*; Marcel Dekker, Inc.: New York, 2000; Vol. *90*.
(40) Zubkov, T.; Smith, R. S.; Engstrom, T. R.; Kay, B. D. Adsorption, Desorption, and Diffusion of Nitrogen in a Model Nanoporous Material. I. Surface Limited Desorption Kinetics in Amorphous Solid Water. *J. Chem. Phys.* **2007**, *127* (18), 184707.
(41) Tait, S. L.; Dohnalek, Z.; Campbell, C. T.; Kay, B. D. N-Alkanes on MgO(100). I. Coverage-Dependent Desorption Kinetics of N-Butane. *J. Chem. Phys.* **2005**, *122*, 16.
(42) Palermo, A.; Aldao, C. Readsorption and Diffusion-Limited TPD of Water from Zeolite Linde 4A. *Thermochim. Acta* **1998**, *319* (1), 177−184.
(43) Palermo, A.; Löffler, D. G. Kinetics of Water Desorption from Pelletized 4A and 5A Zeolites. *Thermochim. Acta* **1990**, *159*, 171−176.
(44) Gorte, R. J. Design Parameters for Temperature Programmed Desorption from Porous Catalysts. *J. Catal.* **1982**, *75* (1), 164−174.
(45) Muhler, M.; Rosowski, F.; Ertl, G. The Dissociative Adsorption of N_2 on a Multiply Promoted Iron Catalyst Used for Ammonia-Synthesis - A Temperature-Programmed Desorption Study. *Catal. Lett.* **1994**, *24* (3−4), 317−331.
(46) Rieck, J. S.; Bell, A. T. Influence of Adsorption and Mass-Transfer Effects on Temperature-Programmed Desorption from Porous Catalysts. *J. Catal.* **1984**, *85* (1), 143−153.
(47) Kanervo, J. M.; Keskitalo, T. J.; Shoor, R. I.; Krause, A. O. I. Temperature-Programmed Desorption as a Tool to Extract Quantitative Kinetic or Energetic Information for Porous Catalysts. *J. Catal.* **2006**, *238* (2), 382−393.
(48) Crooks, R. M.; Yang, H. C.; McEllistrem, L. J.; Thomas, R. C.; Ricco, A. J. Interactions between Self-Assembled Monolayers and an Organophosphonate - Detailed Study Using Surface Acoustic Wave-Based Mass Analysis, Polarization Modulation Ftir Spectroscopy and Ellipsometry. *Faraday Discuss.* **1997**, *107*, 285−305.
(49) Badger, R. M.; Bauer, S. H. Spectroscopic Studies of the Hydrogen Bond. II. The Shift of the O-H Vibrational Frequency in the Formation of the Hydrogen Bond. *J. Chem. Phys.* **1937**, *5* (11), 839−851.
(50) Troya, D.; Edwards, A. C.; Morris, J. R. Theoretical Study of the Adsorption of Organophosphorous Compounds to Models of a Silica Surface. *J. Phys. Chem. C* **2013**, *28*, 14625−14634.